

Phase diagram of hydrogen on Be(0001) from reconstruction-induced surface core-level shifts

Karsten Pohl*

Department of Physics, University of New Hampshire, Durham, New Hampshire 03824, USA

E. Ward Plummer

*Department of Physics and Astronomy, The University of Tennessee, Knoxville, Tennessee 37996, USA
and Solid State Division, Oak Ridge National Laboratories, Oak Ridge, Tennessee 37831, USA*

Søren V. Hoffmann and Philip Hofmann

Institute for Storage Ring Facilities, University of Aarhus, 8000 Aarhus C, Denmark

(Received 15 June 2004; revised manuscript received 13 September 2004; published 29 December 2004)

The surface core-level shifts (SCLS) on the (0001) surface of beryllium were used to study the phase diagram of the hydrogen-induced reconstructions on this surface. Two different top-layer reconstruction phases are formed upon atomic hydrogen adsorption below and above room temperature, respectively. We are able to assign a characteristic core-level spectrum to an individual reconstruction phase and trace its presence at various hydrogen coverages and sample temperatures. This technique makes it possible to survey the low-coverage regions that are lacking long-range ordering. Adsorption of atomic hydrogen in a temperature range of 100 to 270 K induces a $(\sqrt{3} \times \sqrt{3})R30^\circ$ H-Be(0001) chemisorption structure, in which 1/3 of the Be top-layer atoms are removed to form a honeycomb structure of Be vacancies. Upon adsorption above 300 K a (1×3) superstructure forms, which has been proposed to exhibit a missing-row reconstruction of the Be top layer. Our hydrogen-induced SCLS measurements reveal that beryllium vacancies are forming already at small H coverages of 0.2 monolayers.

DOI: 10.1103/PhysRevB.70.235424

PACS number(s): 68.47.De, 68.35.Bs, 79.60.Dp

The study of the adsorption structure of chemisorption systems and the adsorbate-induced surface reconstruction relies mainly on diffraction techniques, such as low-energy electron diffraction (LEED) or x-ray diffraction. In many cases, however, these methods can not be applied because of a lack of long-range ordering especially at low adsorbate coverage regimes. One must resort to local structural probes, like photoelectron diffraction¹ or to spectroscopic techniques, such as electron energy-loss spectroscopy.² In this paper, we present a novel use of surface core-level shifts to deduce the structure of adsorbate systems that do not exhibit long-range periodicity, using hydrogen adsorption on the (0001) surface of beryllium as an example.

The adsorption of atomic hydrogen on Be(0001) leads to two distinct sharp low-energy electron diffraction (LEED) patterns at two different coverages and adsorption temperatures: a $(\sqrt{3} \times \sqrt{3})R30^\circ$ pattern upon adsorption of $\theta=1$ ML at $T_{\text{ads}}=270$ K and three domains of a (1×3) phase upon $2/3$ ML adsorption at 370 K.^{3,4} Both reconstructions dramatically change the geometric surface structure of Be(0001) by forming two superstructures both involving the removal of 1/3 of the Be top-layer atoms. The $(\sqrt{3} \times \sqrt{3})$ phase is made up of a honeycomb structure of Be vacancies, each decorated by three H ad-atoms bonded in tilted bridge sites; according to a recent LEED study³ and in agreement with a density-functional theory (DFT) calculation.⁵ This first-principles study also proposes that at $2/3$ ML coverage the hydrogen atoms are tilted toward linear trenches organized in a $1/3$ Be missing-row structure.^{4,5} A structural I - V analysis of the video LEED data of this phase is underway. The LEED patterns for these two structures, although less in-

tense, are observable in extended regions of the θ vs T phase diagram: The $(\sqrt{3} \times \sqrt{3})$ pattern can be observed in the coverage range between $2/3$ and 1 ML and in a temperature range between 230 to 330 K while the (1×3) pattern is observable between $1/3$ and $2/3$ ML and 270 and 380 K. However, at coverages below $1/3$ ML for $T_{\text{ads}} > 270$ K and below $2/3$ ML for $T_{\text{ads}} < 270$ K only a diffuse (1×1) LEED pattern can be detected. Two conflicting scenarios would explain this behavior: (1) As the DFT calculations predict, the atomic hydrogen adsorbs on a flat, unreconstructed surface and forms a dilute adlayer.⁵ (2) Missing long-range ordering of the reconstructed H-Be chemisorption system at low coverages. In order to resolve the low-coverage adsorption structure one must resort to a local probe such as x-ray photoemission spectroscopy (XPS). The major restructuring of the Be(0001) surface in the two adsorption structures should manifest itself in significant modifications to the $1s$ core-electron binding energies of the beryllium atoms in the surface region, resulting in altered surface core-level shifts (SCLS). The changes will be due to the charge transfer between the adsorbate and the substrate in formation of the chemical bond, and the reconstruction induced change in the surface atom coordination.^{6,7}

In the present study we demonstrate that the adsorbate-induced changes on the SCLS of a clean metal surface can be used as a “fingerprint” of the adsorption geometry at the lowest adsorbate coverages by comparison to the high coverage results for which sharp LEED patterns can be obtained and analyzed. We have studied the effect of hydrogen adsorption on the Be $1s$ level by high-resolution core-level spectroscopy mainly from the structural point of view, by

tracing the fingerprints associated with the two reconstructions across the phase diagram.

The experiments were carried out at the SX700 beam line of the synchrotron radiation source ASTRID in Aarhus, Denmark.⁸ The monochromator was set to give an energy resolution of 70 meV in the photon energy range 135–140 eV. The acceptance angle and energy resolution of the electron analyzer, a VG CLAM-2 hemispherical analyzer with 100 mm mean radius, was chosen to be $\pm 8^\circ$ and 50 meV, respectively. The total energy resolution for this experiment was 86 meV in this photon energy range. All spectra were taken at an incidence angle of 40° and normal emission. The Be(0001) crystal was first mechanically polished, and prepared *in situ* via repeated cycles of 1 keV Ne⁺ bombardment at normal incidence ($10\mu\text{A}/\text{cm}^2$). During the 30 min sputtering the sample was heated to 670 K. Annealing periods of 10 min at 730 K followed each cycle. The sputtering at elevated temperatures facilitated the removal of oxygen. This procedure resulted in a sharp (1×1) LEED pattern and a clean surface as monitored by valence-band and core-level spectroscopy. The sample could be cooled to 150 K via a liquid nitrogen cryostat. Exposing the clean Be(0001) surface to molecular hydrogen does not result in any H or H₂ adsorption in the investigated temperature range. An atomic hydrogen doser was used. It consists of a 0.25 mm tungsten filament heated to 1800 K. The molecular hydrogen was passed through a molybdenum tube of 6 mm diameter surrounding the filament coaxially. The clean Be(0001) surface, located about 3 cm from the end of the Mo tube was thereby exposed to atomic hydrogen. Exposures were controlled by measuring the H₂ background pressure in the chamber; typically some 10^{-7} Torr. The conversion to absolute coverages was done earlier through a nuclear reaction analysis (NRA) experiment. This is an accelerator-based technique in which the proton flux from the reaction $D(^3\text{He},p)^4\text{He}$ on the deuterium covered surface is compared to the p flux from a standard of known deuterium coverage.^{4,9}

At first a photoemission investigation of Be 1s core level from the clean Be(0001) was performed to identify the photon energy at which the intensity of SCLS originating from the first layer is high with respect to the bulk component. Figure 1 displays Be 1s photoemission spectra from Be(0001) as dotted lines recorded at different photon energies in normal emission and at a temperature of 170 K. Four distinct features are resolved, with energy differences large enough to make them out without curve fitting. We assign them as one component from the bulk (B) and three components from the first three layers (S1, S2, S3) in agreement with published work¹⁰ and first principles calculations.¹¹ The relative intensities of the four peaks are strongly dependent on the photon energy. The most important contribution to this energy dependence is given by the inelastic mean free path, which has a minimum at a kinetic energy of 25 eV in beryllium. Therefore the intensity ratio of the first-layer component to lower layer and bulk components is highest for photon energies around 136 eV, i.e., at a kinetic energy of about 25 eV. In the hydrogen adsorption experiments we are mainly interested in the first two layers and have therefore chosen a photon energy of 137.5 eV where the intensity from the B and S3 components are very small.

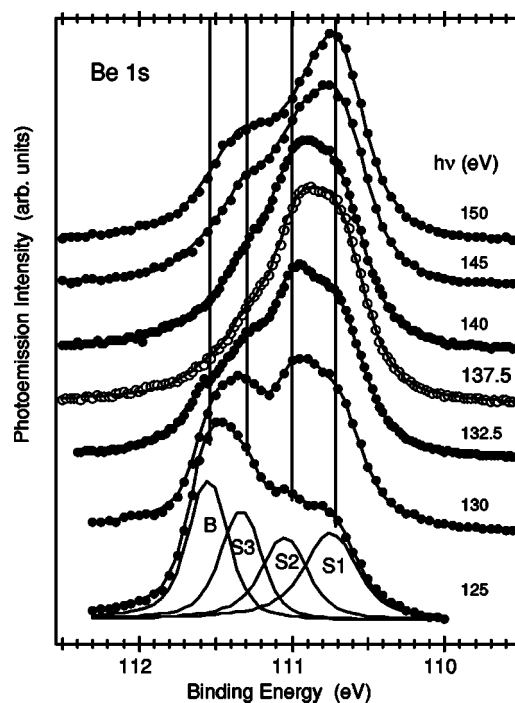


FIG. 1. Be 1s photoemission spectra from Be(0001) recorded at different photon energies in normal emission at 150 K. The solid curves through the data are four component fits. The four peaks shown are fitted to the spectrum taken at 125 eV.

A quantitative analysis of core-level spectra is not a direct process and involves curve-fitting procedures. Doniach-Šunjić line shapes were used with a fixed asymmetry parameter of 0.04 throughout this analysis. It is important to put constraints on the line shapes when fitting four components, and later six, with significant overlap in order to get physical meaningful results. The clean Be(0001) spectra were fitted with a fixed Lorentzian width of 150 meV for the peaks B and S3, 200 meV for S2, and 250 meV for S1 for all photon energies. The Gaussian width depends on the instrumental resolution and is thus energy dependent. It was always kept the same for B, S3, and S2 but increasing with energy from 220 meV at 125 eV to 270 meV at 150 eV. S1 ranged from 240 meV to 280 meV. This variation is consistent with the monochromator resolution in this energy range. These peak widths were determined after a very large number of iterations. The fitted parameters resulted in good fits to the experimental data in the whole photon energy range with a smooth polynomial background.

A fifth component (S4) in the fit in order to account for emission from the fourth layer, as recently suggested by Johansson *et al.*¹² and used in Refs. 13 and 14 was not included. The resolution used in the present experiment hardly justifies another component in the fit and, more importantly, for the photon energy used for the hydrogen adsorption studies the photoemission intensity from the third and lower layers is quite small. We also found that the line shape described above is sufficient to account for the data. No attempts were made to include phonon replicas that have been observed at very high resolution by Andersen *et al.*¹³ However, the relative simplicity of our fitting is not expected to have any influence on the conclusions in this paper.

TABLE I. Surface core-level shifts relative to the Be 1s bulk component observed on Be(0001); energies in meV.

	First layer S1	Second layer S2	Third layer S3
Experiment			
This study	-835 ± 30	-550 ± 35	-245 ± 30
Ref. 10	-825 ± 30	-570 ± 20	-265 ± 25
Theory			
Ref. 11	-870	-600	-220

Within this fixed set of fitting parameters only the peak positions and intensities were varied, which resulted in the curves through the data points shown in Fig. 1 and the following surface shifts relative to the bulk component B: -835 meV (± 30) for S1, -550 meV (± 35) for S2, and -245 meV (± 30) for S3. The error bars give the standard deviation from the independent fit of seven different photon energies. In Table I a comparison with the experiment by Johansson *et al.*¹⁰ and *ab initio* calculations by Feibelman and Stumpf¹¹ is given. The good agreement gives us confidence in the fitting procedure and guarantees the quality of the set of derived parameters that can be used in the following analysis of the H-Be(0001) system. From here on, the clean surface peaks will be fixed in position and only the intensities will be allowed to vary so the evolution of additional hydrogen-induced SCLS can be monitored.

In order to calibrate our results with the LEED observations, the H coverage dependence is investigated at three adsorption temperatures 150 K, 270 K, and 370 K. A first qualitative impression of the H-induced changes in the Be 1s core level is given in Fig. 2(a); it shows a comparison of the clean core-level spectrum with a set of three curves taken at saturation of the (1×3) phase at 2/3 ML ($T_{\text{ads}}=370\text{K}$) and the $(\sqrt{3} \times \sqrt{3})$ structure at 1 ML coverage ($T_{\text{ads}}=270\text{K}$ and 150K). The very different line shapes between each of the two superstructures and the clean Be 1s level are obvious. Comparing the same set of spectra but now recorded at a small hydrogen coverage of 0.2 ML in Fig. 2(b) reveals the same qualitative picture; the spectra taken after adsorption at 150 K and 270 K are identical but significantly different from adsorption at 370 K and the clean spectrum. We find in general at all coverages that the Be 1s core-level spectra taken after adsorbing at 150 K are always identical to the same H coverage adsorbed at 270 K. This leads to a first important conclusion: There are no changes in the phase diagram between 150 K and 270 K.

The coverage dependence for low temperature adsorption is shown in Fig. 3. It displays a series of Be 1s core-level spectra with increasing H coverage for $T_{\text{ads}}=270$ K. Before launching into the quantitative analysis, an important question must be answered: How many hydrogen-induced SCLS should one expect? At saturation the surface is reconstructed in the $(\sqrt{3} \times \sqrt{3})$ honeycomb vacancy structure. Simple counting of the number of inequivalent Be atoms in the first three layers with help from Fig. 4 is intuitive. In the first layer the Be atoms are threefold coordinated, while the sec-

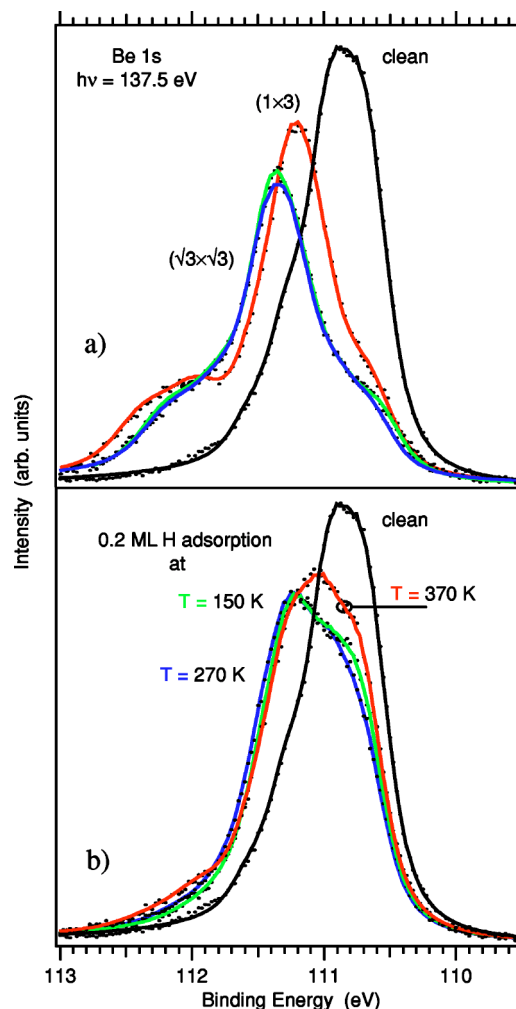


FIG. 2. (Color online) Comparison of the core-level spectrum of the clean surface with (a) a set of three curves; one taken at saturation of the (1×3) phase at 2/3 ML ($T_{\text{ads}}=370\text{K}$) and two taken at $T_{\text{ads}}=270\text{K}$ and 150K at 1 ML hydrogen coverage for the $(\sqrt{3} \times \sqrt{3})$ structure; and with (b) a set of three curves taken at 0.2 ML hydrogen coverage adsorbed at 150 K, 270 K, and 370 K.

ond layer atoms have six nearest neighbors, giving rise to one SCLS per layer. In the third layer, however, 1/3 of the atoms sit underneath the top-layer vacancies while 2/3 are not. Two SCLS emitted from the third layer might be the consequence adding up to a total number of four SCLS from the first three layers. With this number in mind the curve fitting procedure was started. Applying similar constraints to the line shape as in the clean surface case, we find that the core-level spectra can be fitted with six peaks at a fixed position and variable intensity consistently at all hydrogen coverages. The weak bulk (B) and S3 component observed on the clean surface are ignored in the fits because these energy regions turn out to be dominated by two hydrogen-induced peaks H1 and H2. For increasing coverage, the clean S1 and S2 peaks are decreasing continuously, while four hydrogen-induced features grow until saturation. The fitting parameters for S1 and S2 are kept from the fit to the clean core-level spectrum, while the H-induced peaks were fitted as follows: The Lorentzian widths of $H\alpha$, $H\beta$, H1, and H2 were found to

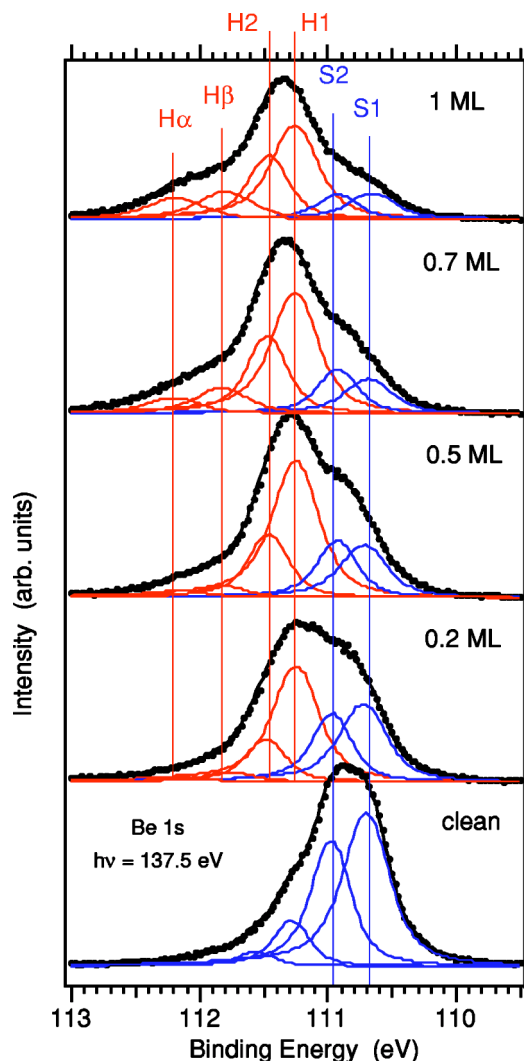


FIG. 3. (Color online) Series of Be 1s core-level spectra taken with increasing H coverage for $T_{\text{ads}}=270$ K. The upper most panel represents saturation of the $(\sqrt{3} \times \sqrt{3})$ LEED pattern.

be 200, 250, 250, and 250 meV, respectively, and the Gaussian widths 230, 260, 260, and 260 meV at all coverages, expect at saturation where H1 and H2 were 350 meV wide. The set of fitting parameters was arrived at after many iterations, so the spectra could be fitted consistently at all coverages with six peaks, two clean surface peaks and four hydrogen-induced SCLS. The extracted shifts relative to the bulk component are given in Table II.

All hydrogen-induced peaks were stationary, i.e., no shift with increasing hydrogen coverage could be detected all the way to saturation, only an increase in peak intensity vs the diminishing clean-surface features S1 and S2. This behavior can be taken as a clear indication that the H-induced structural rearrangement of the surface does not change and that the $(\sqrt{3} \times \sqrt{3})$ honeycomb vacancy reconstruction starts growing already at low coverages. As a consequence and leading to the most important conclusion drawn from this experiment, the vacancy formation of the Be surface does not happen only close to saturation, but already a small number of H adatoms are making the removal of Be top-layer

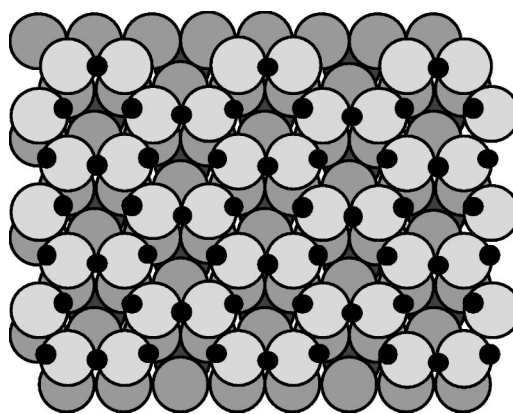


FIG. 4. Top view of the $(\sqrt{3} \times \sqrt{3})R30^\circ$ adsorption structure for 1 ML hydrogen (small circles) on the first three layers (large shaded circles) of the Be(0001). From Ref. 3.

atoms energetically favorable. Small regions of $(\sqrt{3} \times \sqrt{3})$ reconstructed domains will nucleate and grow at the lowest coverages investigated (0.2 ML). In contrast to the first-principle calculation⁵ we see no sign of a dilute phase of H on the unreconstructed surface.

Attempts to assign the four hydrogen-induced SCLS to particular surface atoms did not give reasonable results. An intensity-vs-escape-depth model, which is already problematic in a simple case,¹⁵ is bound to fail for a structure with chemically different atoms in one layer. Moreover, for photon energies lower or higher than 137.5 eV the B and S3 components increase in intensity and can no longer be dismissed as insignificant contributions in the fit. Including them into the fit function would render the fit rather ambiguous. One possible solution to the problem could be photoelectron diffraction experiments at very high resolution but, again, B and S3 would have to be included into the fit. Indeed, any quantitative analysis of the peak areas would require including B and S3 and such an analysis was therefore not attempted here.

For an adsorption temperature of 370 K, the series of Be 1s core-level spectra taken at increasing hydrogen coverage is displayed in Fig. 5. The line shapes are qualitatively different from those in the series taken from the $(\sqrt{3} \times \sqrt{3})$ superstructure. Again, we find that six peaks at fixed positions and variable intensities result in a consistent fit to the spectra for all coverages. Three hydrogen-induced features all with rising intensities, two clean surface peaks S1 and S2 decreasing with H coverage, and the constant bulk component B. The position of the H1 peak coincides with the S3

TABLE II. Hydrogen-induced surface core-level shifts relative to the Be 1s bulk component of the $(\sqrt{3} \times \sqrt{3})$ and (1×3) structure; energies in meV.

	H1	H2	Hβ	Hα
$(\sqrt{3} \times \sqrt{3})$	-292 ± 10	-80 ± 8	$+282 \pm 39$	$+642 \pm 35$
(1×3)	-280 ± 10	$+403 \pm 8$	$+794 \pm 21$	

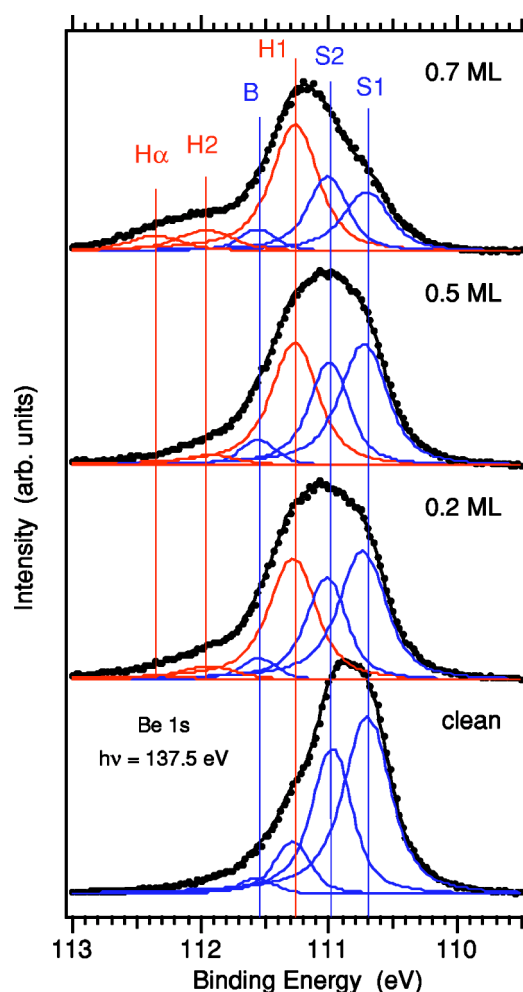


FIG. 5. (Color online) Series of Be 1s core-level spectra taken with increasing H coverage for $T_{\text{ads}}=370$ K. The upper most panel represents saturation of the (1×3) LEED pattern.

component of the clean surface at about 111.3 eV. The convolution of the increasing intensity of the hydrogen-induced feature and the decreasing surface peak explains the apparent initial rise in the peak intensity below 0.2 ML and a much weaker increase between 0.2 ML and 0.7 ML. In the fitting procedure S3 must be ignored for the same reason as in the series taken at 270 K but the bulk component is included because its position does not coincide with any hydrogen-induced features. The fitting parameters for the S1, S2, and B are kept from the fit to the clean core-level spectrum, while the H-induced peaks were fitted as follows: The Lorentzian widths of H1, H2, and H α were found to be 250 meV and the Gaussian widths 260, 350, and 350 meV, respectively, at all coverages. The larger Gaussian widths in this sequence is due to an increased vibrational broadening since the temperature is higher. The higher Gaussian width of H1 and H2 for the $(\sqrt{3} \times \sqrt{3})$ structure at saturation coverage, however, is probably caused by disorder. The extracted shifts relative to the bulk component are given in Table II. Up to saturation of the (1×3) phase at 2/3 ML, all hydrogen-induced peaks are fixed in energy, no shift could be detected, only an in-

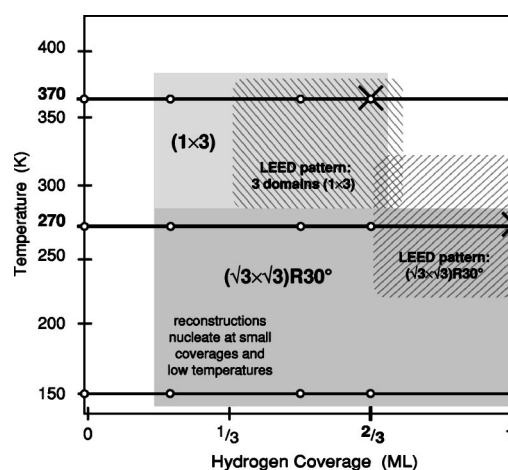


FIG. 6. Phase diagram of the H-Be(0001) chemisorption system from hydrogen-induced SCLS; open circles mark positions where SCLS were analyzed. The LEED pattern in all regions of the phase diagram is (1×1) except in the hatched areas where LEED shows a pattern according to the reconstruction. The bold crosses mark the points in the phase diagram where the sharpest reconstruction-induced diffraction spots can be observed.

crease in peak intensity vs the diminishing clean surface features S1 and S2. This behavior is the same as observed for the $(\sqrt{3} \times \sqrt{3})$ structure and clearly shows that the H-induced surface reconstruction in the (1×3) phase forms already at the lowest coverages investigated.

In summary, the application of high-resolution core-level spectroscopy was successful in exploring the low hydrogen coverage region of the phase diagram by “fingerprinting” the reconstruction phases in a regime where long-range order produce sharp LEED patterns. We find that both H-induced Be(0001) surface reconstructions nucleate at the lowest coverages explored in this experiment; about 0.2 ML. As in the case of the $(\sqrt{3} \times \sqrt{3})$ honeycomb vacancy structure, the removal of Be atoms out of the top-layer can only be weakly thermally activated, because at the lowest investigated adsorption temperature of 150 K the characteristic H-induced SCLS of the vacancy reconstruction were measured. With this surprising results at hand, we are in the position to propose a phase diagram of the hydrogen on Be(0001) chemisorption system, given in Fig. 6. The phase diagram distinguishes two different adsorption structures: (1) Below 280 K in the entire coverage regime up to saturation at 1 ML atomic hydrogen adsorbs in a $(\sqrt{3} \times \sqrt{3})R30^\circ$ honeycomb reconstruction of vacancies in the Be top layer. (2) Hydrogen adsorption above 300 K results in (1×3) reconstruction of the Be surface. This phase saturates at 2/3 ML coverage. Adsorption beyond 2/3 ML hydrogen coverage and above 300 K yield a (1×1) LEED pattern with weak (1×3) and $(\sqrt{3} \times \sqrt{3})$ superstructures spots in the regions indicated. The hydrogen-induced SCLS spectra in this region indicate the coexistence of the two reconstructions. A quantitative analysis, however, was not conclusive and requires a higher instrumental resolution to be able to identify the large number of hydrogen-induced peaks. Experiments using variable-temperature scanning tunneling microscopy will also be undertaken to complement this study.

The authors are grateful to David Adams for making his beam line at ASTRID available for this experiment. This work was supported by NSF-DMR-0105232 and part of this

study was conducted at Oak Ridge National Laboratory, managed by UT-Battelle, LLC, for the U.S. Department of Energy under Contract No. DE-AC05-00OR22725.

*Corresponding author. Email address: karsten.pohl@unh.edu

- ¹D. P. Woodruff, *J. Electron Spectrosc. Relat. Phenom.* **126**, 55 (2002).
- ²H. Ibach and D. Mills, *Electron Energy Loss Spectroscopy* (Academic, New York, 1982).
- ³K. Pohl and E. W. Plummer, *Phys. Rev. B* **59**, R5324 (1999).
- ⁴K. Pohl, Ph.D. thesis, University of Pennsylvania, Philadelphia, 1997.
- ⁵R. Stumpf and P. J. Feibelman, *Phys. Rev. B* **51**, 13 748 (1995).
- ⁶D. Spanjaard, C. Guillot, M.-C. Desjonquères, G. Tréglia, and J. Lecante, *Surf. Sci. Rep.* **5**, 1 (1985).
- ⁷D. M. Riffe, G. K. Wertheim, and P. H. Citrin, *Phys. Rev. Lett.* **65**, 219 (1990).
- ⁸URL: <http://www.isa.au.dk/astrid/astrid.html>
- ⁹D. Dieumegard, D. Dubreuil, and G. Amsel, *Nucl. Instrum. Methods* **166**, 431 (1979).
- ¹⁰L. I. Johansson, H. I. P. Johansson, J. N. Andersen, E. Lundgren, and R. Nyholm, *Phys. Rev. Lett.* **71**, 2453 (1993).
- ¹¹P. J. Feibelman and R. Stumpf, *Phys. Rev. B* **50**, 17 480 (1994).
- ¹²L. I. Johansson, P.-A. Glans, and T. Balasubramanian, *Phys. Rev. B* **58**, 3621 (1998).
- ¹³J. N. Andersen, T. Balasubramanian, C.-O. Almbladh, L. I. Johansson, and R. Nyholm, *Phys. Rev. Lett.* **86**, 4398 (2001).
- ¹⁴A. Baraldi, S. Lizzit, K. Pohl, P. Hofmann, and S. de Gironcoli, *Europhys. Lett.* **64**, 364 (2003).
- ¹⁵S. Lizzit, K. Pohl, A. Baraldi, G. Comelli, V. Fritzsche, E. W. Plummer, R. Stumpf, and P. Hofmann, *Phys. Rev. Lett.* **81**, 3271 (1998).